

Optical coherence tomographic angiography of choroidal neovascularization ill-defined with fluorescein angiography

Mehrdad Malihi, Yali Jia, Simon S Gao, Christina Flaxel, Andreas K Lauer, Thomas Hwang, David J Wilson, David Huang, Steven T Bailey

Casey Eye Institute, Oregon Health & Science University, Portland, Oregon, USA

Correspondence to

Dr Steven Bailey, Casey Eye Institute, Oregon Health & Science University, 3375 SW Terwilliger Blvd, Portland, OR 97239, USA; bailstev@ohsu.edu

Received 26 May 2016

Revised 3 October 2016

Accepted 15 November 2016

ABSTRACT

Purpose To evaluate the morphological structure of ill-defined choroidal neovascularisation (CNV) with traditional fluorescein angiography (FA) compared with optical coherence tomographic angiography (OCTA).

Methods A retrospective case series study of 11 eyes with ill-defined CNV on FA was performed. Eyes were scanned with commercially available spectral-domain optical coherence tomography (OCT) (70 000 A-scans/s). The split-spectrum amplitude-decorrelation angiography (SSADA) algorithm was used to distinguish blood flow from static tissue. En face OCT angiograms were compared with FA.

Results Eleven cases of ill-defined CNV on FA were identified from 10 study participants. Mean age of the participants was 74.5 ± 6.8 years. Six cases had late leakage from undetermined source (LLUS) and five had fibrovascular pigment epithelial detachment (FVPED). Combining cross-sectional structural OCT with OCT angiograms, all cases were found to have type 1 CNV that corresponded to occult CNV with FA. In all cases of occult CNV on FA, distinct vascular structures were visible with OCTA in the outer retinal/retinal pigment epithelium slab. The mean CNV vessel area was $2.61 \pm 3.65 \text{ mm}^2$. The mean CNV vessel area in cases with FVPED was larger than that in cases with LLUS ($4.69 \pm 4.72 \text{ mm}^2$ compared with $0.85 \pm 0.90 \text{ mm}^2$, Mann-Whitney p value=0.04).

Conclusions Although the sample size is small to draw conclusions and the nature of work is retrospective and descriptive, OCTA has the potential to improve visualisation of ill-defined CNV with dye-based angiography, including occult CNV.

Historically, different subtypes of CNV have been defined using FA. Classic CNV is characterised by early hyperfluorescence in a lacy pattern that exhibits expanding areas of increased hyperfluorescence over time. In general, early frames of the FA allow visualisation of CNV tissue and the boundaries of these lesions are well defined, unless obscured by subretinal haemorrhage, which can block fluorescence. An occult CNV, in contrast to classic CNV, has ill-defined boundaries and hyperfluorescence often develops in the later minutes of the angiogram. Occult CNVs are often described as either fibrovascular pigment epithelial detachment (FVPED) or late leakage from undetermined source (LLUS).⁷

Optical coherence tomographic angiography (OCTA) is a novel, non-invasive technique that produces three-dimensional (3D) vascular maps at the microcirculation level. Our group developed the split-spectrum amplitude-decorrelation angiography (SSADA) algorithm, a technique using intensity-based variation over time to identify and quantify blood flow.⁸ SSADA processing can be implemented on spectral-domain (SD) systems without any special hardware modifications. Detection of CNV with SSADA has been reported in AMD, central serous chorioretinopathy and myopia.^{9–18} Without the need of dye, this optical imaging method, OCTA, was hypothesised to provide improved visualisation of CNV. In this manuscript, we compare OCTA with FA in cases where CNV is ill defined with FA, including various types of occult CNV.

METHODS

Study participants were recruited from the retina clinics of Casey Eye Institute, Oregon Health & Science University (OHSU), Portland, Oregon, USA. Informed consent was obtained to undergo OCTA using off-label use of an RTVue-XR Avanti SD-OCT system (Optovue, Fremont, California, USA). The study was planned and conducted in accordance to the principles governing clinical research as set out by the Institutional Review Board at OHSU and the Declaration of Helsinki.

Cases were selected in a retrospective manner by retina specialists (STB and MM) who reviewed the medical records and images of study participants who previously underwent FA and OCTA on the same day between July 2013 and January 2015. FA was obtained with the FF4 fundus camera (Zeiss). Cases were selected if they had ill-defined CNV based on FA.

INTRODUCTION

Neovascular age-related macular degeneration (AMD), characterised by the presence of choroidal neovascularisation (CNV), is a leading cause of vision loss.¹ The detection of CNV is dependent on the use of an intravenous contrast agent, most commonly fluorescein angiography (FA) and less frequently indocyanine green angiography (ICGA).² Both contrast agents are associated with adverse side effects, including anaphylaxis.³ Optical coherence tomography (OCT) provides non-invasive high-resolution images of retinal microstructure and is used to identify exudation associated with CNV. The current management of neovascular AMD uses FA to confirm the presence of CNV while OCT is needed to guide treatment decisions and assess anatomical changes associated with visual potential.^{4–6}



CrossMark

To cite: Malihi M, Jia Y, Gao SS, et al. *Br J Ophthalmol* 2017;**101**:45–50.

OCTA scans were obtained using 840 nm SD-OCT (70 000 A-scans/s) acquiring both 3×3 and 6×6 mm scans. Flow was detected with the SSADA algorithm on both systems as previously described,^{8 17 19} and motion artefact was removed by 3D orthogonal registration and merging of four scans.^{20 21} Cases with poor signal strength or excessive motion artefact were

excluded. Angiograms were exported for custom processing at the Casey Reading Center. Volumetric angiograms were semiautomatically segmented into three layers allowing for separate angiograms of the inner retina, outer retina (location of CNV) and choroid.¹⁸ Shadowgraphic projection artefacts were removed with a slab-subtraction method, reducing inner retinal projection onto the outer retinal angiogram.^{9 17} En face composite angiograms were created, where the inner retinal and outer retinal angiograms were assigned a different colour. The colour-coded angiograms were superimposed on a grey-scale, cross-sectional, structural OCT image to demonstrate blood flow and structural information. The CNV vessel area was calculated by summing pixels with detectable flow in the en face outer retinal angiogram.¹⁷ The Mann-Whitney U test was used to compare the mean CNV vessel area in different subgroups and statistical significance was assumed at $p < 0.05$. Individual cases were analysed with FA and OCTA in a descriptive manner. Images with FA were described as either LLUS or FVPED by the two retinal specialists (STB and MM). The cross-sectional OCTA with both structural and flow information combined was used to classify CNV as above the retinal pigment epithelium (RPE) (type 2) or beneath RPE (type 1).⁷ Three individual cases are discussed comparing and contrasting images with FA and OCTA.

RESULTS

Eleven cases of ill-defined CNV on FA were identified from 10 study participants. The mean age of the participants was 74.5 ± 6.8 years. Six cases had LLUS and five had FVPED. Combining cross-sectional structural OCT with OCT

Table 1 Clinical, fluorescein angiographic and optical coherence tomography angiographic characteristics

Study subject	Age	Treatment status	Scan type	CNV type	CNV vessel area (mm ²)	FA characteristic
1	82	Under treatment	SD-OCT	Type 1	7.12	FVPED
2	89	Under treatment	SD-OCT	Type 1	0.39	FVPED
3	66	Naive	SD-OCT	Type 1	0.84	FVPED
4	70	Under treatment	SD-OCT	Type 1	11.66	FVPED
5	76	Naive	SD-OCT	Type 1	3.48	FVPED
6 OD	73	Naive	SD-OCT	Type 1	1.05	LLUS
6 OS	73	Naive	SD-OCT	Type 1	2.58	LLUS
7	67	Naive	SD-OCT	Type 1	0.42	LLUS
8	69	Naive	SD-OCT	Type 1	0.36	LLUS
9	77	Naive	SD-OCT	Type 1	0.65	LLUS
10	78	Naive	SD-OCT	Type 1	0.08	LLUS

CNV, choroidal neovascularisation; FA, fluorescein angiography; FVPED, fibrovascular pigment epithelial detachment; LLUS, late leakage from undetermined source; OD, Right eye; OS, left eye; SD-OCT, spectral-domain optical coherence tomography.

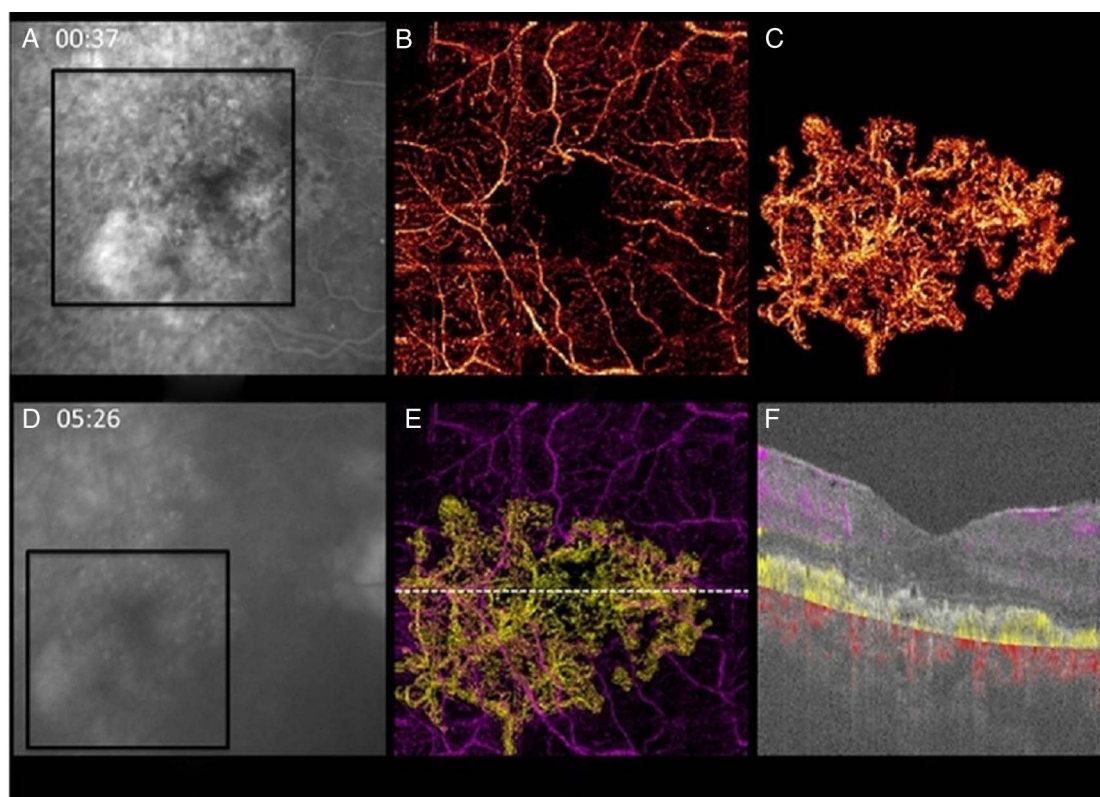


Figure 1 Early (A) and late (D) fluorescein angiography showing an ill-defined region of hyperfluorescence with late staining and leakage. En face spectral-domain optical coherence tomography (OCT) angiogram with inner retinal slab (B, purple in E) and outer retinal/retinal pigment epithelium slab (C, yellow in E) demonstrating large subfoveal choroidal neovascularisation (CNV). Combined cross-sectional OCT with OCT angiogram demonstrating type 1 CNV (yellow) (F).

angiograms, all cases were found to have type 1 CNV that corresponded to occult CNV with FA.

In all cases of occult CNV on FA, distinct vascular structures were visible with OCTA in the outer retinal/RPE slab. Table 1 summarises clinical characteristics along with FA and OCTA findings. The mean CNV vessel area was $2.61 \pm 3.65 \text{ mm}^2$. The mean CNV vessel area in cases that were under treatment was larger than that in treatment-naïve cases ($6.39 \pm 5.67 \text{ mm}^2$ compared with $1.18 \pm 1.20 \text{ mm}^2$, Mann-Whitney p value=0.12), but was not statistically significant. The mean CNV vessel area in cases with FVPED was larger than that in cases with LLUS ($4.69 \pm 4.72 \text{ mm}^2$ compared with $0.85 \pm 0.90 \text{ mm}^2$, Mann-Whitney p value=0.04).

Sample case descriptions

Sample case 1: FVPED visualised by SD-OCTA (study subject no 5)

A 76-year old male, with a visual acuity of 20/20, was diagnosed with an occult CNV with FA. He was asymptomatic and there was no fluid on structural OCT and he was monitored without

treatment for one year. His visual acuity did not change; however, he developed mild metamorphopsia. On the day of OCTA testing, FVPED was present on FA (figure 1A, D). En face SD-OCT angiogram of inner retinal slab and outer retinal slab demonstrated CNV with well-defined boundaries (figure 1B, C, E) correlating to vague area staining and leakage with FA. The CNV vessel calibre appeared larger than primary retinal vessels. The cross-sectional colour overlay demonstrated type 1 CNV (figure 1F).

Sample case 2: LLUS visualised by SD-OCTA (study subject no 6)

A 73-year-old woman noticed vision loss in her left eye (table 1). Visual acuity was 20/30. Drusen, RPE changes and no haemorrhage were noted on clinical examination (figure 2A). Early and late FA images revealed a region of stippled hyperfluorescence that emerges over time consistent with LLUS (figure 2B, C). En face SD-OCTA of $6 \times 6 \text{ mm}$ with colour coding of the inner retina and outer retina demonstrated CNV with a network of vessels extending inferior and nasal to the

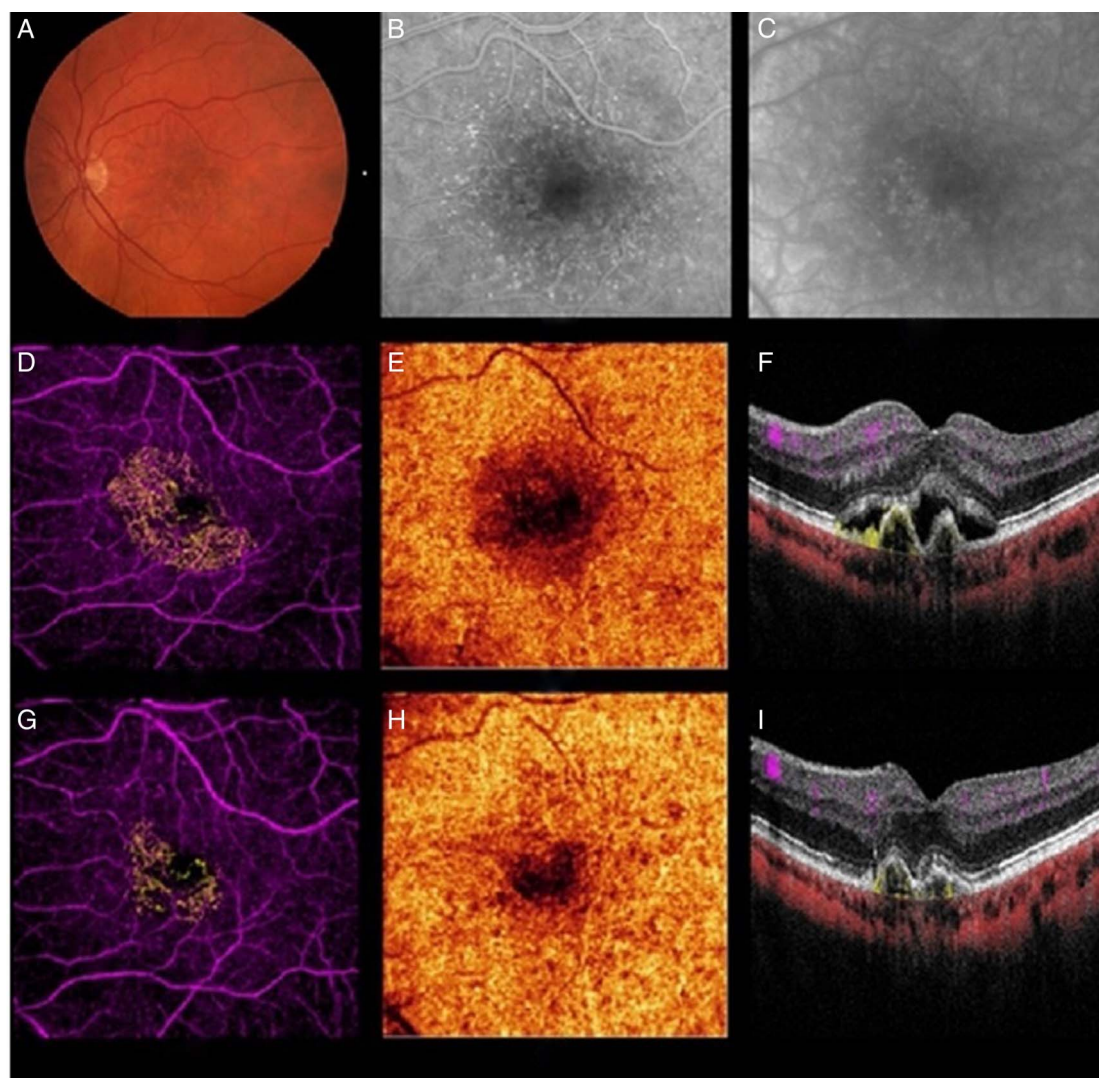


Figure 2 A fundus photo (A). Early (B) and late (C) fluorescein angiography showing a region of stippled hyperfluorescence that emerges over time, inferior and nasal to fovea. (D) $6 \times 6 \text{ mm}$ en face spectral-domain optical coherence tomography (OCT) angiogram of inner retina (purple) and choroidal neovascularisation (CNV) (yellow), clearly visible. (E) Choriocapillaris angiogram demonstrating a relatively confluent signal with a region of reduced signal (flow) identified both underneath and adjacent to the CNV tissue. (F) Cross-sectional, coloured OCT angiogram reveals CNV associated with two small pigment epithelial detachments and subretinal fluid. (G–I) Optical coherence tomographic angiography 1 month after treatment with reduced CNV size and increased signal in the central macular choriocapillaris.

fovea (figure 2D) in the same region of LLUS on FA. This CNV had thin fine vessels arranged in multiple hairpin loop configurations. The combination of cross-sectional structural OCT and OCTA demonstrated type 1 CNV associated with two small pigment epithelial detachments (PEDs) and subretinal fluid (SRF).

Sample case 3: CNV adjacent to serous PED (study subject no 9)

A 77-year-old man experienced decreased vision and distortion in the left eye (table 1). Visual acuity was 20/25 in the left eye and a serous PED with SRF was noted on clinical examination (figure 3A). FA revealed a region of stippled hyperfluorescence adjacent to the serous PED (figure 3B, C). En face SD-OCTA demonstrated CNV adjacent to serous PED (figure 3D). No CNV flow was detected within the serous PED. The cross-sectional structural OCT with flow overlay demonstrated type 1 CNV with several branches extending into the base of the serous PED (figure 3E).

DISCUSSION

In this small series of ill-defined occult CNV with FA, CNV vascular networks could be visualised with OCTA. One limitation of FA is that the RPE blocks fluorescence derived from occult CNV. OCTA does not rely on patterns of fluorescein leakage, instead the 3D volumetric angiograms detect CNV as areas of decorrelation (or flow) in the outer retina, a region devoid of blood flow in healthy eyes. The en face presentation of the volumetric angiogram allows simultaneous visualisation of inner retinal and outer retinal blood flow and, in many cases, CNV branches can readily be distinguished from normal inner retinal circulation. Colour coding the segmented inner retinal and outer retinal slabs helps with CNV identification and localisation.

A unique feature of OCTA compared with FA and ICGA is the ability to present functional blood flow information along with cross-sectional structural OCT. This allows the assessment of relationship of CNV with retinal anatomy in addition to depth-resolved CNV localisation. CNV has been classified histologically by the relationship of CNV with RPE.⁷ OCTA combined with structural OCT allows for in vivo CNV blood flow to be characterised as above or below RPE. In our small series of occult CNV, CNV was identified beneath RPE, consistent with type 1 CNV (table 1). No type 2 or type 3 lesions were found in our series of occult CNV.

In 1984, Gass²² described a series of cases and histological evidence that serous PED with a 'notch sign' with FA was evidence of a hidden occult CNV. He commented that the new vessel formation 'may or may not be evident angiographically'.⁷ In sample case 3 (case no 9 on table 1), FA revealed notched serous PED, with late leakage present in the region of the notch. With OCTA, a type 1 CNV was detected in the region of the notch with branches extending into the serous PED, as Gass postulated.

The detection of CNV by OCTA can be affected by projection artefact and segmentation errors. Projection artefact occurs because moving red blood cells in the superficial vascular structures cast fluctuating shadows into the deeper layers. These shadows vary in amplitude resulting in an artefact decorrelation signal that can be misinterpreted as presence of vessels.^{17 23} RPE has a strong reflectance signal and often inner retinal vessels project onto this layer. Type 1 CNV is closely associated with RPE and it is important to distinguish CNV from projection artefacts, and not to include projection artefacts in CNV vessel area measurements. In our recent work,^{9 17} the flow projection artefact was suppressed with a slab-subtraction algorithm, which means the vascular pattern of inner retinal

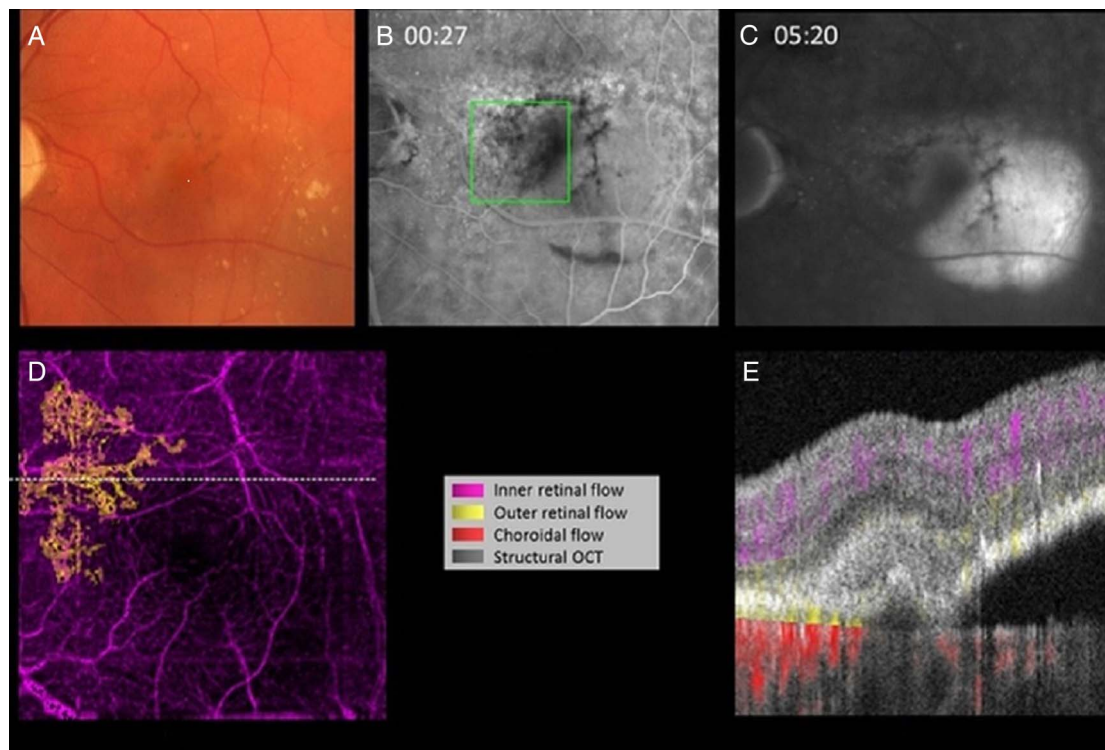


Figure 3 A fundus photo (A) of serous pigment epithelial detachment (PED). Early (B) and late (C) fluorescein angiography (FA) of notched serous PED. En face optical coherence tomography (OCT) angiogram (D) demonstrating choroidal neovascularisation (CNV) in the region of 'notch' on FA. Cross-sectional OCT (E) with angiogram overlay demonstrating type 1 CNV with vessels extending to the margin of the serous PED.

circulation can be subtracted from the outer retinal slab. An additional saliency-based algorithm²⁴ is further needed to completely remove the background clutter by recognising its scattered and disconnected texture.

Segmentation errors occur when pathology disrupts normal anatomical landmarks. Accurate segmentation is important because CNV is distinguished from retinal and choroidal circulation based on depth. In all of the cases in this series, image processing included some degree of manual segmentation to ensure accurate segmentation and manual contouring of CNV vessel area measurements. Manual processing is time-consuming and may be difficult to employ in busy clinical settings. Recently published software improvement using directional graph search segmentation¹⁸ has shown promise to reduce errors and shorten correction times.

CNV vessel area could be determined for all cases of occult CNV, including both FVPED and LLUS. Change in CNV size with ICGA has been reported to be useful in evaluating treatment response with an anti-vascular endothelial growth factor therapy.²⁵ OCTA-based CNV vessel area calculations may provide a non-invasive way to monitor CNV size while undergoing treatment.²⁶ In sample case 2 (case 6 on table 1) on table 1), after a single treatment with bevacizumab, the CNV vessel area decreased from 2.56 to 1.54 mm² and peripheral CNV branches disappeared. A choriocapillaris angiogram demonstrated a relatively confluent signal with a region of reduced signal (flow) identified both underneath and adjacent to the CNV tissue and after treatment some, but not all, of the choriocapillaris flow appeared to return. Others have noted the reduced choriocapillaris perfusion adjacent to CNV.^{10 27} In this case, the choriocapillaris flow appeared to improve after treatment was given. A steal phenomenon has been proposed to explain observed changes in choriocapillaris flow in the setting of CNV: flow from choriocapillaris is shunted to CNV, so as CNV vascular channels get shut down due to treatment, choriocapillaris flow subsequently returns. An alternative explanation is, as SRF resolves and retinal thickness is reduced with treatment, the OCT signal at the choriocapillaris improves and choriocapillaris is better visualised.

In this small study, we selected a variety of clinical cases of ill-defined CNV on FA. In these cases, OCTA allowed discrimination of CNV boundaries and depth, along with en face localisation. This study is limited by its small sample size, and its retrospective and descriptive nature. Given these limitations, conclusions comparing FA and OCTA are limited. However, this study supports the role of OCTA and provides insight contrasting the differences between OCTA and FA. Compared with FA, OCTA has several known attributes that are favourable, including faster acquisition time and the avoidance of possible complications with an invasive intravenous dye. Therefore, large-scale validation studies are needed to further define the role of OCTA in ill-defined CNV on FA in the clinical setting.

Contributors All authors made substantial contributions to the conception and design of the work, the acquisition, analysis and interpretation of data, drafting of the work and revising it critically for important intellectual content. All authors provided final approval of the version published and are in agreement to be accountable for all aspects of the work in ensuring that questions related to the accuracy or integrity of any part of the work are appropriately investigated and resolved.

Funding (a) National Institute of Health grants: R01-EY024544, DP3-DK104397, R01-EY023285 and P30-EY010572. (b) Research to Prevent Blindness Unrestricted/Challenge (U/C) Grant.

Competing interests Oregon Health & Science University (OHSU), YJ and DH have a significant financial interest in Optovue, a company that may have a commercial interest in the results of this research and technology. DH has a significant financial interest in Carl Zeiss Meditec. These potential conflicts of interest have been reviewed and managed by OHSU. The other authors have no conflict of interest or relevant financial disclosure.

Ethics approval The Institutional Review Board at OHSU.

Provenance and peer review Not commissioned; externally peer reviewed.

REFERENCES

- Congdon N, O'Colmain B, Klaver CC, *et al.* Causes and prevalence of visual impairment among adults in the United States. *Arch Ophthalmol* 2004;122:477–85.
- Bressler N, Bressler SB, Fine SL. Age-related macular degeneration. *Surv Ophthalmol* 1988;32:375–413.
- Yannuzzi LA, Rohrer KT, Tindell LJ, *et al.* Fluorescein angiography complication survey. *Ophthalmology* 1986;93:611–17.
- Brown DM, Kaiser PK, Michels M, *et al.* Ranibizumab versus verteporfin for neovascular age-related macular degeneration. *N Engl J Med* 2006;355:1432–44.
- Martin DF, Maguire MG, Fine SL, *et al.* Ranibizumab and bevacizumab for treatment of neovascular age-related macular degeneration: two-year results. *Ophthalmology* 2012;119:1388–98.
- Heier JS, Brown DM, Chong V, *et al.* Intravitreal aflibercept (VEGF trap-eye) in wet age-related macular degeneration. *Ophthalmology* 2012;119:2537–48.
- Gass JD. *Stereoscopic atlas of macular diseases: diagnosis and management*. St. Louis: Mosby, 1997.
- Jia Y, Tan O, Tokayer J, *et al.* Split-spectrum amplitude-decorrelation angiography with optical coherence tomography. *Opt Express* 2012;20:4710–25.
- Jia Y, Bailey ST, Hwang TS, *et al.* Quantitative optical coherence tomography angiography of vascular abnormalities in the living human eye. *Proc Natl Acad Sci USA* 2015;112:E2395–402.
- Moult E, Choi W, Waheed NK, *et al.* Ultrahigh-speed swept-source OCT angiography in exudative AMD. *Ophthalmic Surg Lasers Imaging Retina* 2014;45:496–505.
- Spaide RF. Optical coherence tomography angiography signs of vascular abnormalization with antiangiogenic therapy for choroidal neovascularization. *Am J Ophthalmol* 2015;160:6–16.
- Coscas G, Lupidi M, Coscas F, *et al.* Optical coherence tomography angiography during follow-up: qualitative and quantitative analysis of mixed type I and II choroidal neovascularization after vascular endothelial growth factor trap therapy. *Ophthalmic Res* 2015;54:57–63.
- de Carlo TE, Bonini Filho MA, Chin AT, *et al.* Spectral-domain optical coherence tomography angiography of choroidal neovascularization. *Ophthalmology* 2015;122:1228–38.
- Teusink MM, Breukink MB, van Grinsven MJ, *et al.* OCT angiography compared to fluorescein and indocyanine green angiography in chronic central serous chorioretinopathy. *Invest Ophthalmol Vis Sci* 2015;56:5229–37.
- Mastropasqua R, Di Antonio L, Di Staso S, *et al.* Optical coherence tomography angiography in retinal vascular diseases and choroidal Neovascularization. *J Ophthalmol* 2015;2015:343515.
- Palejwala NV, Jia Y, Gao SS, *et al.* Detection of nonexudative choroidal neovascularization in age-related macular degeneration with optical coherence tomography angiography. *Retina (Philadelphia, Pa)* 2015;35:2204–11.
- Jia Y, Bailey ST, Wilson DJ, *et al.* Quantitative optical coherence tomography angiography of choroidal neovascularization in age-related macular degeneration. *Ophthalmology* 2014;121:1435–44.
- Zhang M, Wang J, Pechauer AD, *et al.* Advanced image processing for optical coherence tomographic angiography of macular diseases. *Biomed Opt Express* 2015;6:4661–75.
- Gao SS, Liu G, Huang D, *et al.* Optimization of the split-spectrum amplitude-decorrelation angiography algorithm on a spectral optical coherence tomography system. *Opt Lett* 2015;40:2305–8.
- Kraus MF, Potsaid B, Mayer MA, *et al.* Motion correction in optical coherence tomography volumes on a per A-scan basis using orthogonal scan patterns. *Biomed Opt Express* 2012;3:1182–99.
- Kraus MF, Liu JJ, Schottenhaml J, *et al.* Quantitative 3D-OCT motion correction with tilt and illumination correction, robust similarity measure and regularization. *Biomed Opt Express* 2014;5:2591–613.
- Gass JD. Serous retinal pigment epithelial detachment with a notch. A sign of occult choroidal neovascularization. *Retina* 1984;4:205–20.
- Spaide RF, Fujimoto JG, Waheed NK. Image artifacts in optical coherence tomography angiography. *Retina (Philadelphia, Pa)* 2015;35:2163–80.

- 24 Liu L, Gao SS, Bailey ST, *et al.* Automated choroidal neovascularization detection algorithm for optical coherence tomography angiography. *Biomed Opt Express* 2015;6:3564–76.
- 25 Rush RB, Rush SW, Aragon AV II, *et al.* Evaluation of choroidal neovascularization with indocyanine green angiography in neovascular age-related macular degeneration subjects undergoing intravitreal bevacizumab therapy. *Am J Ophthalmol* 2014;158:337–44.
- 26 Kuehlewein L, Bansal M, Lenis TL, *et al.* Optical coherence tomography angiography of type 1 neovascularization in age-related macular degeneration. *Am J Ophthalmol* 2015;160:739–48.e2.
- 27 Coscas GJ, Lupidi M, Coscas F, *et al.* Optical coherence tomography angiography versus traditional multimodal imaging in assessing the activity of exudative age-related macular degeneration: a new diagnostic challenge. *Retina (Philadelphia, Pa)* 2015;35:2219–28.